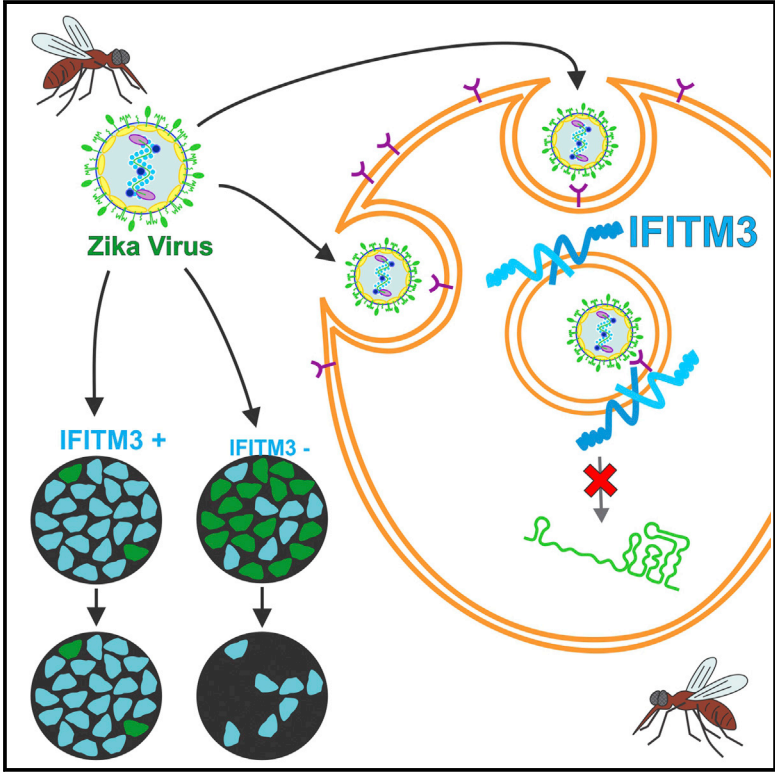# Cell Reports

The IFITMs Inhibit Zika Virus Replication

Graphical Abstract

Authors

George Savidis, Jill M. Perreira,
Jocelyn M. Portmann, Paul Meraner,
Zhiru Guo, Sharone Green,
Abraham L. Brass

Correspondence

abraham.brass@umassmed.edu

In Brief

Savidis et al. find that the IFITMs block Zika virus replication, including that of a recently isolated strain from Cambodia. Importantly, this protection translates into a large reduction in Zika-virus-induced cell death. The authors develop an imaging assay and determine that IFITM3 blocks the very earliest stages of Zika virus infection.

Highlights

- IFITM3 and IFITM1 inhibit Zika virus infection

- IFITM3 can prevent Zika-virus-induced cell death

- The IFITMs can halt Zika virus early in the viral life cycle

CrossMark

CellPress

Report

The IFITMs Inhibit Zika Virus Replication

George Savidis,[1] Jill M. Perreira,[1] Jocelyn M. Portmann,[1] Paul Meraner,[1] Zhiru Guo,[2] Sharone Green,[2]
and Abraham L. Brass[1,3,*]
[1]Department of Microbiology and Physiological Systems (MaPS), University of Massachusetts Medical School, Worcester, MA 01655, USA
[2]Division of Infectious Diseases and Immunology, Department of Medicine, University of Massachusetts Medical School, Worcester,
MA 01655, USA
[3]Division of Gastroenterology, Department of Medicine, University of Massachusetts Medical School, Worcester, MA 01655, USA
*Correspondence: abraham.brass@umassmed.edu
http://dx.doi.org/10.1016/j.celrep.2016.05.074

SUMMARY

Zika virus has emerged as a severe health threat with a rapidly expanding range. The IFITM family of restriction factors inhibits the replication of a broad range of viruses, including the closely related flaviruses West Nile virus and dengue virus. Here, we show that IFITM1 and IFITM3 inhibit Zika virus infection early in the viral life cycle. Moreover, IFITM3 can prevent Zika-virus-induced cell death. These results suggest that strategies to boost the actions and/or levels of the IFITMs might be useful for inhibiting a broad range of emerging viruses.

INTRODUCTION

Zika virus has emerged as a severe health threat by virtue of its fast paced global spread and its associated morbidities, including microcephaly and Guillain-Barre syndrome (D'Ortenzio et al., 2016; Driggers et al., 2016; Haug et al., 2016; Lazear and Diamond, 2016; Musso and Gubler, 2016; Rasmussen et al., 2016). Zika virus was initially isolated from an infected macaque in Uganda in 1947, and the first human cases were reported in 1952. Similar to the closely related dengue virus, Zika virus is primarily spread via the bite of an infected Aedes mosquito. In 2007, Zika virus emerged in Micronesia and expanded its range to Southeast Asia. Zika virus was identified in Brazil in May 2015 and has since led to widespread infection in Central and South America.

Zika virus illness has been described as self-limited and moderate in severity with the common findings of malaise, headache, fever, joint aches, a maculopapular rash, and inflammation of the conjunctiva (Haug et al., 2016; Lazear and Diamond, 2016). However, an alarming number of birth defects, including microcephaly, have been attributed to Zika virus infection occurring in the first two trimesters of pregnancy (Driggers et al., 2016; Haug et al., 2016; Rasmussen et al., 2016). In addition, an upsurge in reported cases of Guillain-Barre syndrome, which manifests as a symmetric ascending flaccid paralysis, have recently been associated with Zika virus infection. Multiple reports have demonstrated that Zika virus can be sexually transmitted via infected seminal fluid, with resultant infection of pregnant mothers; the risk of sexual transmission may persist for months after remission of clinical illness (D'Ortenzio et al., 2016). These events

have led to Zika virus being declared a public health emergency by the World Health Organization.

We and others have found that the small membrane-associated interferon-inducible transmembrane proteins (IFITMs) can inhibit the replication of a wide range of pathogenic viruses, including all flaviviruses tested to date, including West Nile virus, dengue virus, and reporter viruses carrying the envelope of the Omsk hemmorhagic fever virus (Bailey et al., 2014; Brass et al., 2009; Chesarino et al., 2014a, 2014b, 2015; Everitt et al., 2012; Huang et al., 2011; Perreira et al., 2013; Tartour et al., 2014). Murine models of Zika virus pathogenesis require an absence of type I interferon (IFN) signaling, suggesting that IFN-stimulated genes (ISGs) can prevent heightened levels of infection (Lazear et al., 2016). Further evidence for the protective role of ISGs comes from work showing that placental cells can resist Zika virus infection due to actions of IFN-λ (Bayer et al., 2016). In light of these data, and given that IFITMs are potent inhibitors of flaviviral infection, we wished to determine their effect on Zika virus replication. Using both loss- and gain-of-function examples, we found that both IFITM3 and IFITM1 inhibit the replication of a prototype lab strain of Zika virus first isolated in Africa in 1947 (MR766) (Dick et al., 1952), as well as a more recent strain isolated from a child in Cambodia in 2010 (FSS13025) (Haddow et al., 2012). We found IFITM3 to be more potent than IFITM1 in its inhibition of Zika virus replication. Consistent with this, the loss of a specific endocytosis motif required for the proper localization of IFITM3 is necessary for maximal viral restriction (Jia et al., 2014; John et al., 2013). We also revealed that Zika virus causes a cytopathic effect in HeLa cells and that IFITM3 modulates this phenotype. These data examine the role that specific ISGs might play in the intrinsic immune system's defenses against Zika virus and further extend the important role played by the IFITMs against viral infection. Our data, and those of others, also suggest that methods of enhancing the actions of IFITMs could serve to ameliorate the global impact on human health created by the expansion of Zika virus, as well as the challenges posed by other emerging viral infections.

RESULTS

IFITM3 Modulates Zika Virus Replication and Cytopathicity

In view of the established role of the IFITMs in the anti-viral response against multiple flaviviruses, we wished to examine the effect of IFITM3 on Zika virus infection (Brass et al., 2009;
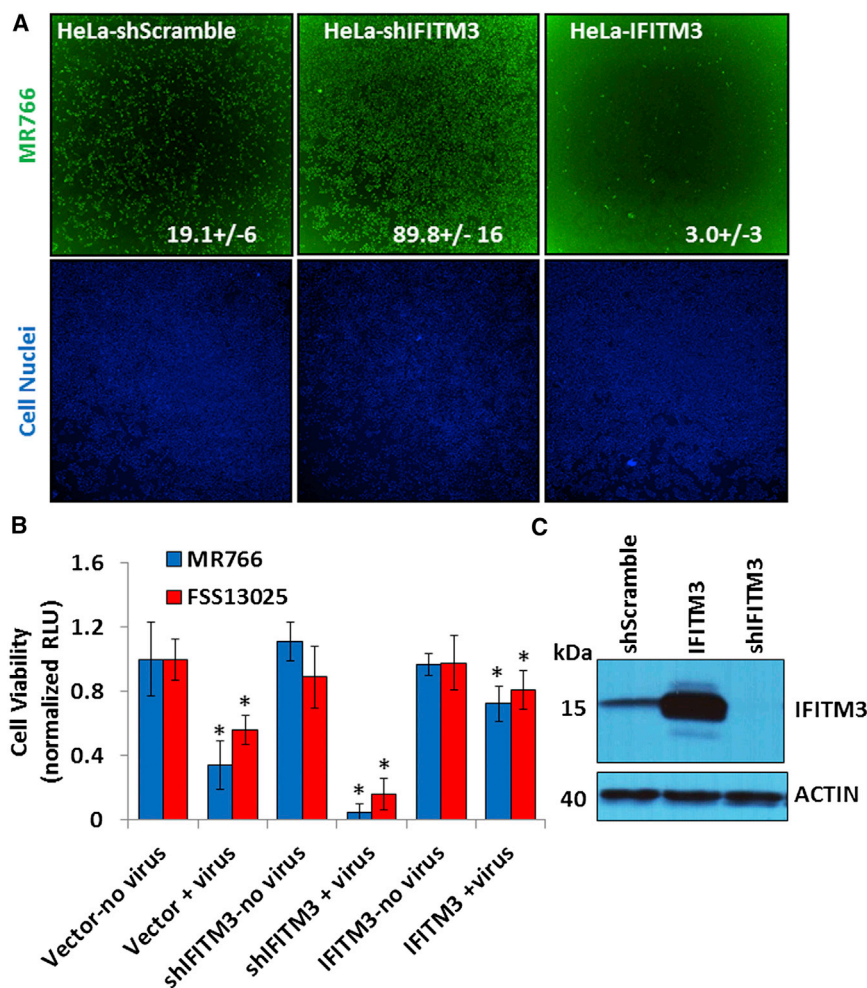
Figure 1. IFITM3 Modulates Zika Virus Replication and Cytopathicity

(A) HeLa cells were plated at equal numbers and infected 24 hr later with Zika virus MR766 (Uganda, 1947) at an MOI of 0.2. At 48 hr after infection, the cells were fixed, permeabilized, and immunostained for the viral envelope (E) protein using monoclonal antibody 4G2 (green). The nuclei of the cells were also stained for DNA with Hoechst 33342 dye (blue). Imaging analysis software was used to determine the percentage infection (numbers shown ± SD) and the number of nuclei. 4× magnification.

(B) HeLa cell lines were plated at equal numbers and infected 24 hr later with Zika virus strain MR766 or FSS13025 at an MOI of 1. 3 days later, the cells were incubated with Cell Titer Glo and the relative light units were recorded and normalized to the control shScramble uninfected samples.

(C) Immunoblots of the lysates from the cells used in (A) and (B) using the indicated antibodies. Actin serves as a loading control. kDa, kilodalton.

Values in (A) and (B) indicate the mean of n = 3 independent experiments ± SD. *$p \leq 0.05$ (Student's t test).

caused the death of HeLa cells and whether the loss or gain of IFITM3 impacted this effect. We found that there was a moderate amount of cell death detected after Zika virus infection of the shScramble control cells and that this effect was ameliorated with overexpression of IFITM3 (Figures 1B and 1C). Importantly, the loss of IFITM2 and IFITM3 (shIFITM3 cells) enhanced the susceptibility of the cells to viral cytopathic effect. We saw similar results when using both the MR766 and FSS13025 strains, with the MR766 strain displaying a stronger cytopathic effect. We conclude that IFITM2 and IFITM3 are required for cellular resistance to Zika virus replication and cytopathicity and that the overexpression of IFITM3 can potentiate this protection.

John et al., 2013). We found that depletion of IFITM3 via a stably transduced short hairpin RNA (shIFITM3) in human cervical carcinoma (HeLa) cells increased Zika virus replication as demonstrated by increased expression of Zika-virus envelope (E) protein staining with a flavivirus cross-reactive antibody that recognizes the E protein, 4G2 (Figure 1A). We obtained similar results by assessing viral double-stranded RNA (dsRNA) with a recombinant J2 (rJ2) monoclonal antibody (data not shown). In keeping with these results, IFITM3-overexpressing cells potently blocked viral infection as compared to the shScramble control cells (Figure 1A). We note that the shIFITM3 used in this study spares IFITM1 expression but targets a nearly identical region of both IFITM2 and IFITM3, which differ by only 11 amino acids (Figure S1A) (Feeley et al., 2011; Perreira et al., 2013). Furthermore, we have not found an antibody that can discriminate between endogenous IFITM2 and IFITM3, therefore the increased susceptibility of the shIFITM3 cells to Zika virus infection represents the depletion of both endogenous IFITM2 and IFITM3, with the latter likely playing the predominant role (see Discussion).

Zika virus infection has been reported to cause the death of Vero cells but not of human or murine fibroblasts (Way et al., 1976). We therefore wanted to confirm that Zika virus infection

IFITM1 Inhibits Zika Virus Replication, and the Proper Localization of IFITM3 Is Needed for Its Full Restriction of Viral Replication

We next tested whether overexpression of the IFITM3 paralog, IFITM1, impacted Zika virus replication. IFITM1 and IFITM3 have been shown to have partially overlapping specificities of viral inhibition, with IFITM1 being more potent against viruses that enter at the cell surface or in the early endosomal pathway and IFITM3 preferentially acting more strongly against viruses that enter in the late endosomal pathway, such as dengue virus or influenza A virus (Bailey et al., 2014; Chesarino et al., 2014b; Perreira et al., 2013). In keeping with these observations, overexpressed IFITM1 did inhibit Zika virus replication (MR766 and FSS13025 strains), but to a lesser extent than IFITM3, with the caveat that we cannot compare the levels of these two untagged proteins directly (Figures 2A–2C). An IFITM3
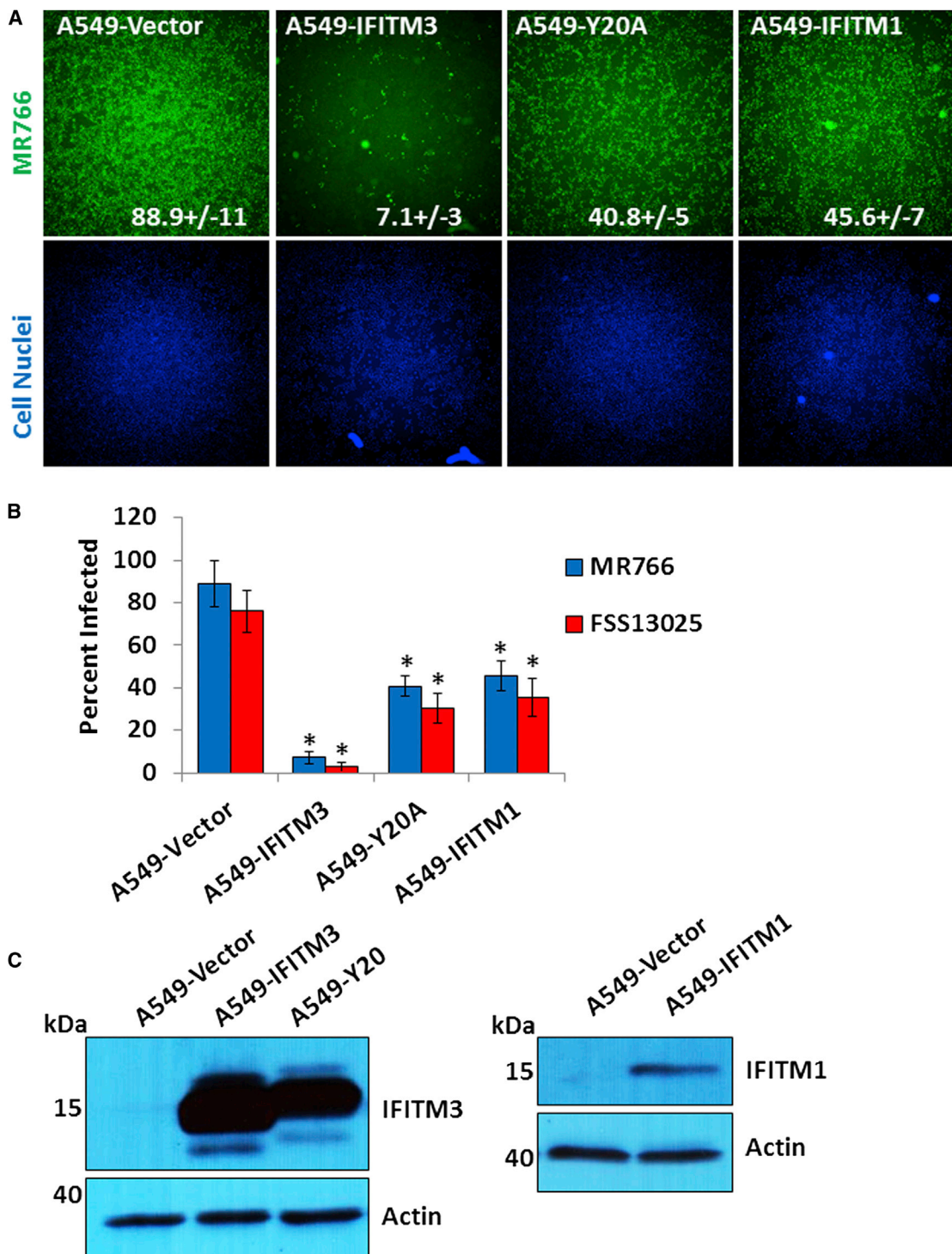
Figure 2. IFITM1 Inhibits Zika Virus Replication and the Proper Localization of IFITM3 Is Needed for Its Full Restriction of Viral Replication

(A and B) A549 cell lines were plated at equal numbers and infected 24 hr later with either Zika virus MR766 (Uganda, 1947) or FSS13025 (Cambodia, 2010) at an MOI of 1. At 48 hr after infection, the cells were fixed, permeabilized, and immunostained for viral dsRNA (green). The nuclei of the cells were also stained for DNA with Hoechst 33342 dye (blue). Imaging analysis software was used to determine the percentage infection (numbers shown ± SD) and the number of nuclei. Values indicate the mean percentage of infected cells of n = 3 independent experiments ± SD. 4× magnification. *p ≤ 0.05 (Student's t test).

(C) Immunoblots of the lysates from the cells used in (A) and (B) using the indicated antibodies. Actin serves as a loading control. kDa, kilodalton.
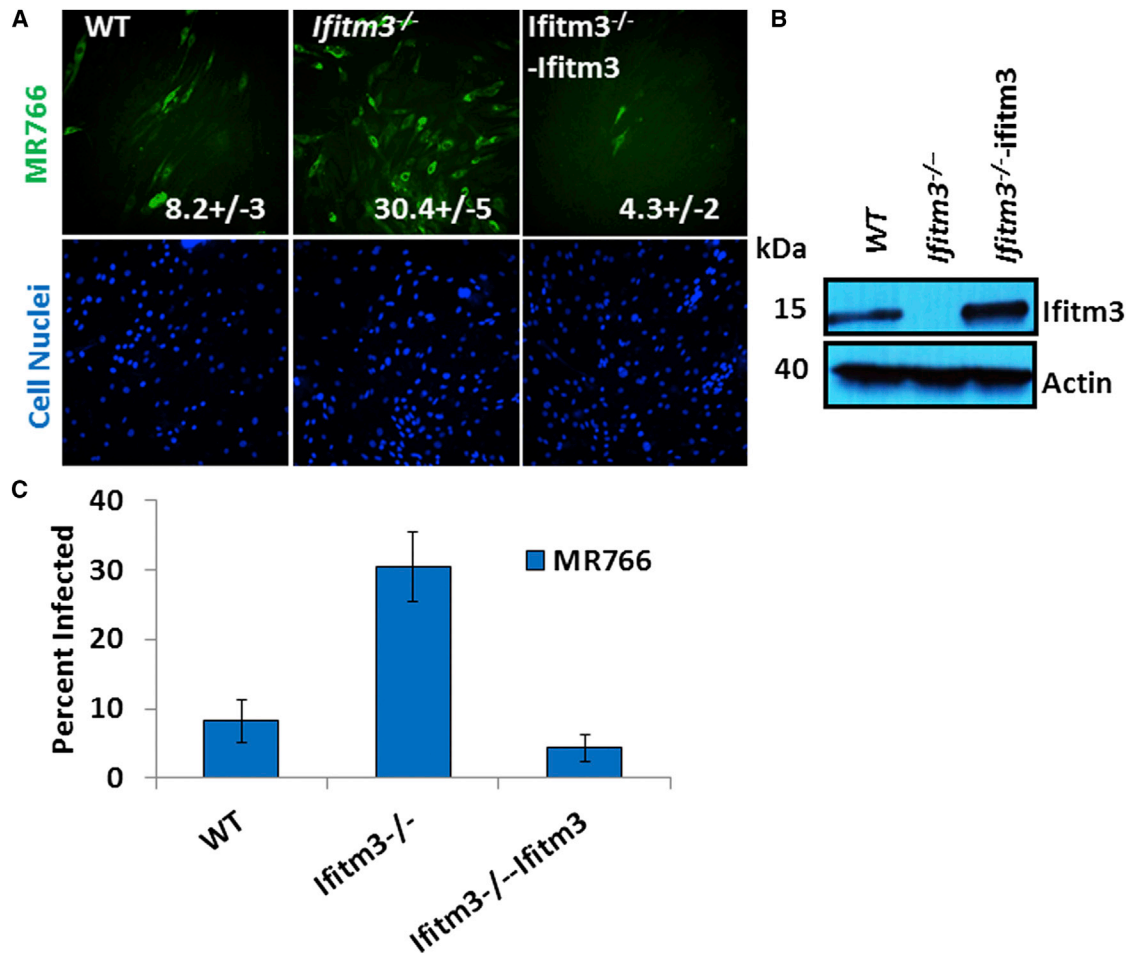
Figure 3. Deletion of the Murine *Ifitm3* Locus Leads to Increased Zika Virus Infection In Vitro
(A) The indicated MEF cell lines were incubated with Zika virus FSS13025 (Cambodia, 2010) at an MOI of 0.2. 48 hr later the cells were fixed, permeabilized, and immunostained for the viral E protein (green). The nuclei of the cells were also stained for DNA with Hoechst 33342 dye (blue). Imaging analysis software was used to determine the percentage of infection and the number of nuclei. Values indicate the mean percent infected cells of n = 3 independent experiments ± SD. 20× magnification.
(B) Immunoblots of the lysates from the cells used in (A) using the indicated antibodies. Actin serves as a loading control. kDa, kilodalton.
(C) Quantitation of cells in (A), with values indicating the mean percentage of infected cells of n = 3 independent experiments ± SD.

mutant, Y20A, which harbors a mutation in a clathrin-mediated endocytosis motif required for proper protein localization in the endosomal pathway, also demonstrated a moderately reduced ability to block viral replication (Jia et al., 2014; John et al., 2013).

Deletion of the Murine *Ifitm3* Locus Leads to Increased Zika Virus Infection In Vitro
Murine Ifitm3 has been shown to prevent viral replication in vitro and also to stop severe influenza in vivo (Brass et al., 2009; Everitt et al., 2012; Feeley et al., 2011). Therefore, we compared *Ifitm*$^{3+/+}$, *Ifitm*$^{3-/-}$, and *Ifitm*$^{3-/-}$Ifitm3 mouse embryonic fibroblasts (MEFS) in the setting of Zika virus infection (MR766 strain), with the latter null cells complemented *in trans* with a stably transduced murine Ifitm3 cDNA (Lin et al., 2013). These studies revealed an increase in infection in the *Ifitm3*$^{-/-}$ cells, which was prevented by exogenously expressed Ifitm3 (Figures 3A–

3C). We conclude that Ifitm3 protects mouse cells from Zika infection, similar to its role in human cells.

IFITM3 Inhibits the Early Stages of Zika Virus Replication
The IFITMs have been shown to restrict viral replication by blocking fusion-pore formation and the entry of the viral genome and its associated proteins into the cytosol (Bailey et al., 2014; Brass et al., 2008; Feeley et al., 2011; Li et al., 2013; Lin et al., 2013; Perreira et al., 2013). Therefore, we tested whether altering the levels of IFITM3 could inhibit the early stages of Zika virus infection by using an imaging assay we designed to detect Zika virus RNA. Zika virus (MR766, MOI 50–100) was incubated on ice with HeLa-shScramble, -shIFITM3, and -IFITM3 cells to permit viral binding but prevent endocytosis. Warm media was then added, and at the indicated time points, the cells were washed with cold PBS, incubated with or without trypsin, fixed, immunostained, and confocally imaged with a probe set that recognizes Zika
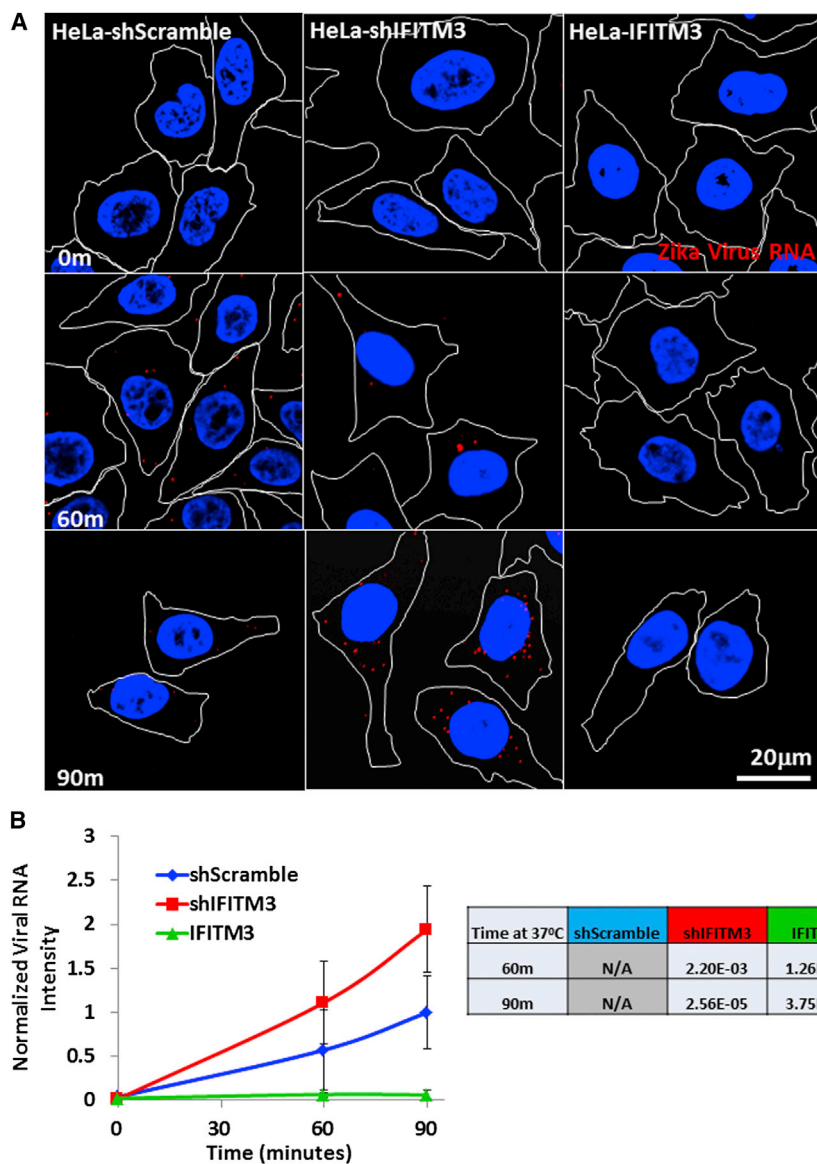
A

B

Time at 37ºC	shScramble	shIFITM3	IFITM3
60m	N/A	2.20E-03	1.26E-04
90m	N/A	2.56E-05	3.75E-05

Figure 4. IFITM3 Inhibits the Early Replication of Zika Virus

(A) HeLa cell lines were incubated on ice with Zika virus MR766 (Uganda, 1947) at an MOI of 100. At time zero, warm media was added and the cells were fixed, permeabilized, and stained for Zika virus RNA (red) and confocally imaged so as to capture a centrally located area within the cells. The nuclei of the cells were also stained for DNA with Hoechst 33342 dye (blue). White lines outline the cell boundaries based on DIC imaging. 63× magnification.

(B) Quantitation of the intensity of the viral RNA signals in cells in (A), normalized to the shScramble control cells. Values indicate the mean intensity of the red viral RNA signals of n = 3 independent experiments ± SD. A Student's t test was used to calculate the indicated p value shown in the table.

Of note, at time zero we saw no differences in viral binding (either in signal intensity or number) to the cell surface across the three cell lines when using samples that were incubated with virus then immediately fixed and immunostained for viral E protein (Figures S1C–S1F). We also estimate that the larger "spots" of viral signals (E protein and viral RNA) represent multiple viruses or viral RNAs that are close together and beyond the resolution of this assay, which is 360 nm for the E protein and 400 nm for the viral RNA. Therefore, with individual Zika viruses estimated to be ≈50 nm in size, our imaging assays are not capable of discriminating between individual virions and are thus useful for evaluating the relative level of viral signals rather than their absolute numbers. Taken together, these studies reveal that IFITM3 inhibits the early stages of Zika virus infection that occur after viral-host binding but before either the viral RNA's cytosolic entry or its early transcription.

virus RNA. We found that the loss of IFITM3 resulted in increased viral RNA signals (in terms of both intensity and number) as compared to the shScramble control cells (Figures 4A and 4B, Figure S1B). Consistent with this, the overexpression of IFITM3 resulted in little to no detectable viral RNA signals in the cytosol. Given that IFITM3 prevents the fusion of multiple viruses, these results suggest that this assay only recognizes viral RNA once it has exited the viral particle and entered the cytosol subsequent to fusion-pore formation; attempts to detect viral RNA fixed to the cell surface in time-zero samples not treated with trypsin showed little to no viral RNA signal, supporting this notion (data not shown). However, we cannot rule out the possibility that some viral RNA transcription occurred at these early time points post-infection, and thus it remains possible that the IFITMs act after viral fusion but prior to early viral RNA transcription.

DISCUSSION

Zika virus has emerged as a threat to global health, with the most severe effects being seen in resource-limited areas (Lazear and Diamond, 2016; Musso and Gubler, 2016; Rasmussen et al., 2016). Therefore it is important to learn all that we can about preventing and treating Zika virus infections. Toward that goal, we have tested the effect of the anti-viral proteins, IFITM3 and IFITM1, on Zika virus replication.

These studies showed that both IFITM1 and IFITM3 inhibit Zika virus infection. Moreover, IFITM3 is likely the more potent of the two restriction factors when cells encounter Zika virus, and its effect is dependent on its proper localization within the

endosomal pathway. Although the shIFITM3 used in this work targets both IFITM2 and IFITM3, the *Ifitm3*$^{-/-}$ MEF studies argue that IFITM3 plays the predominant role in blocking Zika virus replication. These findings are in keeping with our earlier studies that revealed the anti-viral actions of the IFITMs against the closely related flaviviruses West Nile virus and dengue virus (Brass et al., 2009; John et al., 2013). Together, these data clearly demonstrate that IFITMs are potent inhibitors of several major emerging viruses and as such warrant further investigation into strategies to enhance their levels and/or actions. Further studies using *Ifitm*-deficient mice to assess the in vivo implications of these findings are warranted (Everitt et al., 2012; Lange et al., 2008).

IFITM3 has been shown to be required to prevent influenza A virus infections in both humans and mice (Bailey et al., 2012; Brass et al., 2009; Everitt et al., 2012; Lin et al., 2013; Perreira et al., 2013). Individuals homozyogous for the IFITM3 allele, rs12252-C, are at increased risk of severe influenza (Everitt et al., 2012; Yang et al., 2015; Zhang et al., 2013). While rare in individuals of European ancestry, the rs12252-C allele is more prevalent in Asia and Micronesia. Given the recent expansion of Zika virus into these regions, it will be of interest to determine whether this allele is also a risk factor for more severe infections in both mothers and fetuses and whether this might in any way contribute to the risk of Zika-virus-associated birth defects.

Our data show that IFITM3 inhibits the early stages of Zika virus replication. The exact mechanism of IFITM-mediated restriction is unknown; however, the results of orthologous experimental approaches suggest that the IFITMs directly alter the properties of the cell and/or viral membrane, resulting in a block to fusion-pore formation (Brass et al., 2009; Desai et al., 2014; Feeley et al., 2011; Li et al., 2013; Lin et al., 2013; Perreira et al., 2013; Tartour et al., 2014). Given that our studies show that IFITM3 elicits a profound decrease in the early intracellular levels of Zika virus RNA, a similar mechanism of action most likely underlies this inhibition. IFITM3's relatively higher basal level of expression as compared to IFITM1, together with its early block to viral replication, suggests that IFITM3 may provide an important initial defense against Zika virus infection, prior to the induction of a full complement of ISGs. More work is now required to better understand how the flaviviruses are blocked by the IFITMs in the hope that this knowledge can be used to prevent and treat a broad range of expanding viral infections that now threaten human health.

EXPERIMENTAL PROCEDURES

Cells and Culture Conditions
TZM-bl HeLa cells (Figures 4 and S1, NIH AIDS Reagent Repository no. 8129, from John Kappes and Xiaoyun Wu), H1 HeLa cells (Figure 1, ATCC), and Vero (ATCC) and A549 cells (ATCC) were grown in complete DMEM (Sigma) with 10% fetal bovine serum (FBS; Invitrogen) and 2 mM L-glutamine (Invitrogen).

Viruses
Zika virus strains were kindly provided by Robert Tesh at the World Reference Center for Emerging Viruses and Arboviruses at the University of Texas Medical Branch in Galveston, Texas: FSS13025, isolated from a patient in Cambodia in 2010 (Haddow et al., 2012) and MR766, originally obtained from a Rhesus macaque in Uganda in 1947. Zika viruses were propagated in Vero cells (ATCC) (Dick et al., 1952), and the titer was determined by standard

plaque assays and immunofluorescence imaging assays for E protein expression (Brass et al., 2009; John et al., 2013).

Plasmids
The following shRNA sequence (sense strand, shIFITM3) was cloned into the pLK0.1 shRNA puro lentiviral vector to create retroviruses used to stably transduce cells as described (Feeley et al., 2011): 5′-CCTCATGACCATTCTGCT CATC-3′. Alignment of this shRNA sequence with IFITM3 is as follows:

```
shIFITM3   CCTCATGACCATTCTGCTCATC
           ||||||||||||||||||||||
IFITM3     CCTCATGACCATTCTGCTCATC
```

Alignment with IFITM2 is as follows:

```
shIFITM3   CCTCATGACCATTCTGCTCATC
           | |||||||||||||||||||
IFITM2     CTTCATGACCATTCTGCTCATC
```

Alignment with IFITM1 is as follows:

```
shIFITM3   CCTCATGACCATTCTGCTCATC
           |||||||||||||    |||||
IFITM1     CCTCATGACCATTGGATTCATC
```

MEFs
Adult *Ifitm3*$^{+/-}$ mice were intercrossed, and MEFs were derived from embryos at day 13.5 of gestation to produce homozygous *Ifitm3*$^{-/-}$ and the matching wild-type control MEFs (Everitt et al., 2012). The stable exogenous expression of Ifitm3 in the null cells has been previously described (Everitt et al., 2012). MEFs were cultured in DMEM with the addition of MEM, non-essential amino acids, sodium pyruvate, 2-Mercapto-ethanol (GIBCO), and 15% FBS and 2mM L-glutamine.

Cell Viability Assays
Equivalent numbers of H1 HeLa cells (HeLa-shScramble, -shIFITM3, or -IFITM3) were plated on white 96-well plates (Corning) and 24 hr later were infected with either Zika virus MR766 Uganda 1947 or Zika virus FSS13025 Cambodia 2010 at an MOI of 1. After 3 days of infection, the plates were removed from the incubator and after equilibration to room temperature, Cell Titer Glo reagent was added (diluted 1:16 in D-PBS). After 20 min incubation, the relative light units were read with a Luminoskan Ascent Microplate Luminometer (Thermo Fisher, kindly provided by Peter DiStefano, Elixir Pharmaceuticals).

Immunoblotting
Whole-cell lysates were prepared with Laemmeli buffer and resolved by SDS-PAGE. The samples were then transferred to Immobilon-P membrane (Millipore) and probed with the indicated antibodies. Anti-IFITM3 anti-sera (Abgent, AP1153a) was used at 1:250. Anti-IFITM3 from Abcam (Anti-Fragilis (ab15592)) was used at 1:500. Anti-IFITM1 (Proteintech, catalog no. 60074-1-Ig) was used at 1:1,000. Actin (Sigma, catalog no. A2228-200UL) was used at 1:5,000. Secondary anti-Rabbit HRP conjugated antibody (Jackson Immuno Research, 211-062-171) and anti-mouse HRP conjugated antibody (Jackson Immuno Research, 115-035-003) were used at 1:10,000.

Immunofluorescence Studies
Cells were fixed in 4% formalin (Sigma) in D-PBS (Sigma) for 10 min, followed by a wash with D-PBS. Blocking was performed for 30 min in 1% BSA (BioPharm, 71-010) in D-PBS containing 0.3 M glycine (Sigma, G7126). Cells were next incubated in the 4G2 hybridoma supernatant diluted 1:2 (clone D1-4G2-4-15; Millipore, MAB10216) or recombinant J2 (rJ2) anti-dsRNA antibody (Kerafast, ES2001) in 1% BSA in D-PBS for at least 1 hr, followed by three washes with D-PBS. Cells were then incubated with secondary antibodies Alexa Fluor Goat anti-mouse 488 (Life Technologies, A11001) diluted 1:1,000 in D-PBS containing 1% BSA. Cells were washed three times with D-PBS before being mounted to slides using Vectashield with DAPI (4′, 6′-di-amidino-2-phenylindole) (Vector Laboratories, H-1200). Samples were then imaged with either a confocal microscope or an Image Xpress Micro (IXM)

scanning microscope. Using a pinhole of 0.9 a.u. on the confocal microscope, the resolution of the imaging assay for viral E protein and viral RNA is 360 nm in the 488 channel (E protein) and 400 nm in the 550 channel (viral RNA); flaviviruses are estimated to be 50 nm, so we are not able to discriminate individual virions by using this confocal microscope. All microscope settings were kept constant throughout the entirety of a given experiment.

Zika Virus RNA Imaging Assay

Cells were fixed in 4% formalin in D-PBS for 10 min, followed by a wash with D-PBS. The staining was done with the QuantiGene ViewRNA ISH Assay Kit (Panomics, Affymetrix, QVC0001) and a Zika virus RNA probe (Panomics, Affymetrix, VF1-19981). Samples were permeabilized in 1× detergent (Panomics, Affymetrix) (10× stock diluted in PBS) for 5 min at room temperature, followed immediately with two washes in 1× PBS. Samples were then treated with protease (Panomics, Affymetrix) diluted 1:1,000 in 1× PBS for 15 min at room temperature, then immediately washed three times with 1× PBS. Zika virus probe set was diluted 1:50 in pre-warmed (40°C) probe set diluent and added to samples which were then incubated at 40°C for 3 hr in a humidified chamber. Samples were washed three times with ViewRNA wash buffer (Panomics, Affymetrix). Pre-Amp was diluted 1:25 in pre-warmed (40°C) amplifier diluent and added to samples for 30 min at 40°C in a humidified chamber. Samples were washed three times with ViewRNA wash buffer. Amp was diluted 1:25 in pre-warmed (40°C) amplifier diluent and added to samples for 30 min at 40°C in a humidified chamber. Samples were washed three times with ViewRNA wash buffer. Label probe was diluted 1:25 in pre-warmed (40°C) label probe diluent and added to samples for 30 min at 40°C in a humidified chamber. Samples were washed three times with ViewRNA wash buffer before being mounted to slides using Vectashield with DAPI (4', 6'-diamidino-2-phenylindole) (Vector Laboratories, H-1200).

Confocal Image Quantification

Fluorescence intensity was quantified with FIJI software. The intensity was measured as the average fluorescence intensity per cell. First, the image file was opened in the FIJI software, and the cell to be measured was outlined with the "freehand selections" tool to define the ROI (region of interest), using the differential interference contrast (DIC) image as a guide. After setting the ROI, the intensity was quantified with the measure tool (selected from Analyze > Measure). Next, a region outside of the cells was selected to determine the background fluorescence of the image. The measured values were then recorded into a Microsoft Excel file for further analysis. The intensity value measured for the cell had the background intensity subtracted to obtain the net intensity for the cell. Multiple cells (n > 12) for each condition were measured and the average ± SD of the net intensity was calculated for each condition across the experiment. To make differences across the conditions easier to appreciate, the average net intensity values were then normalized to the control condition of each experiment by dividing the average and SD for each condition by the average of the control condition. Data were then represented graphically.

Zika Virus E Protein and Viral RNA Signal Quantification

12-bit multichannel images were opened with the free online software program FIJI. The cell of interest was outlined with the freehand selections tool, using the DIC channel as a guide. The threshold was set to a minimum of 900 and maximum of 4,096 for the viral staining (E protein or viral RNA). The number of individual foci was quantified with the analyze particles tool (Analyze > Analyze Particles). The size range of counted foci was 1-infinity pixels, to remove background in the quantification. Foci counts per cell were recorded for all cells in each condition (≥ 12 cells per condition per experiment) in a Microsoft Excel document and represented as a bar graph using the mean and SD.

SUPPLEMENTAL INFORMATION

Supplemental Information includes one figure and can be found with this article online at http://dx.doi.org/10.1016/j.celrep.2016.05.074.

REFERENCES

Bailey, C.C., Huang, I.C., Kam, C., and Farzan, M. (2012). Ifitm3 limits the severity of acute influenza in mice. PLoS Pathog. 8, e1002909.

Bailey, C.C., Zhong, G., Huang, I.C., and Farzan, M. (2014). IFITM-family proteins: the cell's first line of antiviral defense. Annu. Rev. Virol. 1, 261–283.

Bayer, A., Lennemann, N.J., Ouyang, Y., Bramley, J.C., Morosky, S., Marques, E.T., Jr., Cherry, S., Sadovsky, Y., and Coyne, C.B. (2016). Type III Interferons Produced by Human Placental Trophoblasts Confer Protection against Zika Virus Infection. Cell Host Microbe 19, 705–712.

Brass, A.L., Dykxhoorn, D.M., Benita, Y., Yan, N., Engelman, A., Xavier, R.J., Lieberman, J., and Elledge, S.J. (2008). Identification of host proteins required for HIV infection through a functional genomic screen. Science 319, 921–926.

Brass, A.L., Huang, I.C., Benita, Y., John, S.P., Krishnan, M.N., Feeley, E.M., Ryan, B.J., Weyer, J.L., van der Weyden, L., Fikrig, E., et al. (2009). The IFITM proteins mediate cellular resistance to influenza A H1N1 virus, West Nile virus, and dengue virus. Cell 139, 1243–1254.

Chesarino, N.M., McMichael, T.M., Hach, J.C., and Yount, J.S. (2014a). Phosphorylation of the antiviral protein interferon-inducible transmembrane protein 3 (IFITM3) dually regulates its endocytosis and ubiquitination. J. Biol. Chem. 289, 11986–11992.

Chesarino, N.M., McMichael, T.M., and Yount, J.S. (2014b). Regulation of the trafficking and antiviral activity of IFITM3 by post-translational modifications. Future Microbiol. 9, 1151–1163.

Chesarino, N.M., McMichael, T.M., and Yount, J.S. (2015). E3 Ubiquitin Ligase NEDD4 Promotes Influenza Virus Infection by Decreasing Levels of the Antiviral Protein IFITM3. PLoS Pathog. 11, e1005095.

D'Ortenzio, E., Matheron, S., de Lamballerie, X., Hubert, B., Piorkowski, G., Maquart, M., Descamps, D., Damond, F., Yazdanpanah, Y., and Leparc-Goffart, I. (2016). Evidence of Sexual Transmission of Zika Virus. N. Engl. J. Med. Published online April 13, 2016. http://dx.doi.org/10.1056/NEJMc1604449.

Desai, T.M., Marin, M., Chin, C.R., Savidis, G., Brass, A.L., and Melikyan, G.B. (2014). IFITM3 restricts influenza A virus entry by blocking the formation of fusion pores following virus-endosome hemifusion. PLoS Pathog. 10, e1004048.

Dick, G.W., Kitchen, S.F., and Haddow, A.J. (1952). Zika virus. I. Isolations and serological specificity. Trans. R. Soc. Trop. Med. Hyg. 46, 509–520.

Driggers, R.W., Ho, C.Y., Korhonen, E.M., Kuivanen, S., Jääskeläinen, A.J., Smura, T., Rosenberg, A., Hill, D.A., DeBiasi, R.L., Vezina, G., et al. (2016). Zika Virus Infection with Prolonged Maternal Viremia and Fetal Brain Abnormalities. N. Engl. J. Med. Published online March 30, 2016. http://dx.doi.org/10.1056/NEJMoa1601824.

Everitt, A.R., Clare, S., Pertel, T., John, S.P., Wash, R.S., Smith, S.E., Chin, C.R., Feeley, E.M., Sims, J.S., Adams, D.J., et al.; GenISIS Investigators; MOSAIC Investigators (2012). IFITM3 restricts the morbidity and mortality associated with influenza. Nature *484*, 519–523.

Feeley, E.M., Sims, J.S., John, S.P., Chin, C.R., Pertel, T., Chen, L.M., Gaiha, G.D., Ryan, B.J., Donis, R.O., Elledge, S.J., and Brass, A.L. (2011). IFITM3 inhibits influenza A virus infection by preventing cytosolic entry. PLoS Pathog. *7*, e1002337.

Haddow, A.D., Schuh, A.J., Yasuda, C.Y., Kasper, M.R., Heang, V., Huy, R., Guzman, H., Tesh, R.B., and Weaver, S.C. (2012). Genetic characterization of Zika virus strains: geographic expansion of the Asian lineage. PLoS Negl. Trop. Dis. *6*, e1477.

Haug, C.J., Kieny, M.P., and Murgue, B. (2016). The Zika Challenge. N. Engl. J. Med. *374*, 1801–1803.

Huang, I.C., Bailey, C.C., Weyer, J.L., Radoshitzky, S.R., Becker, M.M., Chiang, J.J., Brass, A.L., Ahmed, A.A., Chi, X., Dong, L., et al. (2011). Distinct patterns of IFITM-mediated restriction of filoviruses, SARS coronavirus, and influenza A virus. PLoS Pathog. *7*, e1001258.

Jia, R., Xu, F., Qian, J., Yao, Y., Miao, C., Zheng, Y.M., Liu, S.L., Guo, F., Geng, Y., Qiao, W., and Liang, C. (2014). Identification of an endocytic signal essential for the antiviral action of IFITM3. Cell. Microbiol. *16*, 1080–1093.

John, S.P., Chin, C.R., Perreira, J.M., Feeley, E.M., Aker, A.M., Savidis, G., Smith, S.E., Elia, A.E., Everitt, A.R., Vora, M., et al. (2013). The CD225 domain of IFITM3 is required for both IFITM protein association and inhibition of influenza A virus and dengue virus replication. J. Virol. *87*, 7837–7852.

Lange, U.C., Adams, D.J., Lee, C., Barton, S., Schneider, R., Bradley, A., and Surani, M.A. (2008). Normal germ line establishment in mice carrying a deletion of the Ifitm/Fragilis gene family cluster. Mol. Cell. Biol. *28*, 4688–4696.

Lazear, H.M., and Diamond, M.S. (2016). Zika Virus: New Clinical Syndromes and Its Emergence in the Western Hemisphere. J. Virol. *90*, 4864–4875.

Lazear, H.M., Govero, J., Smith, A.M., Platt, D.J., Fernandez, E., Miner, J.J., and Diamond, M.S. (2016). A Mouse Model of Zika Virus Pathogenesis. Cell Host Microbe *19*, 720–730.

Li, K., Markosyan, R.M., Zheng, Y.M., Golfetto, O., Bungart, B., Li, M., Ding, S., He, Y., Liang, C., Lee, J.C., et al. (2013). IFITM proteins restrict viral membrane hemifusion. PLoS Pathog. *9*, e1003124.

Lin, T.Y., Chin, C.R., Everitt, A.R., Clare, S., Perreira, J.M., Savidis, G., Aker, A.M., John, S.P., Sarlah, D., Carreira, E.M., et al. (2013). Amphotericin B increases influenza A virus infection by preventing IFITM3-mediated restriction. Cell Rep. *5*, 895–908.

Musso, D., and Gubler, D.J. (2016). Zika Virus. Clin. Microbiol. Rev. *29*, 487–524.

Perreira, J.M., Chin, C.R., Feeley, E.M., and Brass, A.L. (2013). IFITMs restrict the replication of multiple pathogenic viruses. J. Mol. Biol. *425*, 4937–4955.

Rasmussen, S.A., Jamieson, D.J., Honein, M.A., and Petersen, L.R. (2016). Zika Virus and Birth Defects–Reviewing the Evidence for Causality. N. Engl. J. Med. *374*, 1981–1987.

Tartour, K., Appourchaux, R., Gaillard, J., Nguyen, X.N., Durand, S., Turpin, J., Beaumont, E., Roch, E., Berger, G., Mahieux, R., et al. (2014). IFITM proteins are incorporated onto HIV-1 virion particles and negatively imprint their infectivity. Retrovirology *11*, 103.

Way, J.H., Bowen, E.T., and Platt, G.S. (1976). Comparative studies of some African arboviruses in cell culture and in mice. J. Gen. Virol. *30*, 123–130.

Yang, X., Tan, B., Zhou, X., Xue, J., Zhang, X., Wang, P., Shao, C., Li, Y., Li, C., Xia, H., and Qiu, J. (2015). Interferon-Inducible Transmembrane Protein 3 Genetic Variant rs12252 and Influenza Susceptibility and Severity: A Meta-Analysis. PLoS ONE *10*, e0124985.

Zhang, Y.H., Zhao, Y., Li, N., Peng, Y.C., Giannoulatou, E., Jin, R.H., Yan, H.P., Wu, H., Liu, J.H., Liu, N., et al. (2013). Interferon-induced transmembrane protein-3 genetic variant rs12252-C is associated with severe influenza in Chinese individuals. Nat. Commun. *4*, 1418.